



# The New 2018 Version of the Meudon Spectroheliograph

J.-M. Malherbe<sup>1</sup> · K. Dalmasse<sup>2</sup>

© Springer ●●●

**Abstract** Daily full-disk observations of the solar photosphere and chromosphere started at Meudon Observatory in 1908. After a review of the scientific context and the historical background, we describe the instrumental characteristics and capabilities of the new version operating since 2018. The major change is the systematic recording of full line profiles over the entire solar disk providing 3D data cubes. Spectral and spatial sampling are both improved. Classical 2D images of the Sun at fixed wavelength are still delivered. We summarize the different processing levels of on-line data and briefly review the new scientific perspectives.

**Keywords:** photosphere; chromosphere; spectroheliograph; full-sun; long-term observations

## 1. Introduction

Systematic observations of the solar disk started at the Meudon Observatory in 1908 with Deslandres spectroheliograph. The collection is one of the largest available to the international community with ten observed cycles (observations were only interrupted during the First World War). It contains mainly monochromatic images in wavelengths as H $\alpha$  (center), CaII K1v (violet wing) and CaII K3 (center). A few spectroheliographs were built at about the same time at Mount Wilson (USA: Hale, 1907; Bertello, Ulrich, and Boyden, 2010), Kodaikanal (India: Hasan *et al.*, 2010) and Coimbra (Portugal: Garcia *et al.*, 2011). The Meudon and Coimbra spectroheliographs are still in use.

Most present full-disk observations of the Sun are performed with narrow band imagers such as Fabry P erot filters (e.g. Global Oscillation Network Group H $\alpha$  network: Harvey *et al.*, 2011) or Lyot filters (e.g. Global H $\alpha$  Network: Gallagher *et al.*, 2002). Spectroheliographs, however, operate in spectroscopic mode and

---

<sup>1</sup> LESIA, Observatoire de Paris, 92195 Meudon, and PSL Research University, France, email: Jean-Marie.Malherbe@obspm.fr

<sup>2</sup> IRAP, Universit e de Toulouse, CNRS, CNES, UPS, 31028 Toulouse, France, email: Kevin.Dalmasse@irap.opm.eu

the 2018 release provides 3D data cubes  $(x, y, \lambda)$ ,  $\lambda$  being the wavelength along line profiles and  $(x, y)$  the spatial coordinates on the Sun.

This work is for the purpose of promoting the studies requiring full-disk spectral data and/or long-term observations. Section 2 recalls the scientific interest of long-term archives in solar physics. In Section 3, we present an historical background summarizing the evolutions of the Meudon spectroheliograph from the end of the 19th century up to now. Section 4 describes the instrumental characteristics and capabilities of the 2018 version. The data taken with the new spectrograph are widely open to the community as explained in Section 5. Finally, Section 6 discusses new perspectives.

## 2. Scientific Context of Spectroheliograms and Long-Term Observations

The 110-year-old Meudon collection contains full-disk spectroheliograms that are relevant to research on the solar cycle, activity, and space weather. CaII K1v data make it possible to analyze photospheric properties of active regions (ARs), while H $\alpha$  reveals solar filaments. Such data are used to produce synoptic maps of sunspots, faculae, and filaments (Martres and Zlicaric, 1982), and monthly publications (D’Azambuja, 1920) in *l’Astronomie* during the 1928–2003 period. This in turn provides information on the evolution of solar structures during the cycle, including the equatorward migration of ARs (Makarov and Sivaraman, 1989; Mouradian and Soru-Escout, 1993; Charbonneau, 2010) and the poleward migration of high-latitude filaments (Mouradian and Soru-Escout, 1994; Karna, Pesnell, and Zhang, 2015).

Sunspot number and area derived from full-disk CaII K1v observations, as well as filament number and length derived from H $\alpha$ , further characterize the amplitude, duration, and activity level of the solar cycle (Schwabe, 1844; Wolf, 1861; Hale *et al.*, 1919; Hoyt and Schatten, 1998; Hathaway, Wilson, and Reichmann, 2002; Petrovay, 2010). Quiescent H $\alpha$  filaments delineate large cells of opposite magnetic polarities, which allowed Leroy, Bommier, and Sahal-Brechot (1983) to suggest different topologies of prominence magnetic support. When analyzed over long periods, data series help to study the cycle-to-cycle variability (long-term modulations such as the Gleissberg cycle or grand minima such as the Maunder minimum: see the review by Hathaway, 2010).

Long-term collections of full-disk observations provide constraints to improve our understanding of the solar dynamo and its variations (*e.g.* Tobias, 2002; Norton, Charbonneau, and Passos, 2014). Mein and Ribes (1990) used some structures of spectroheliograms (spots and faculae) as magnetic tracers to delineate large-scale motions. Ribes and Bonnefond (1990) found the presence of zonal meridional circulation at several latitudes suggesting rolls below the surface.

Full-disk CaII K1v and H $\alpha$  centennial archives are also useful to study extreme solar flares such as the Carrington event (Carrington, 1859; Hodgson, 1859) or the two-ribbon flare of 25 July 1946 (Ellison, 1946). The largest sunspot region ever seen was registered on 05 April 1947, and it challenged researchers on the maximum size of groups (Aulanier *et al.*, 2013). Studying extreme events requires

long-term archives that contribute to the development of prediction tools for space weather applications (Schrijver *et al.*, 2012; Schmieder, 2018).

Several works have proposed new proxies to extract information from archives. Pevtsov *et al.* (2016) developed a proxy to derive magnetic flux in the plage and sunspots from CaII spectroheliograms. This proxy will be important for pseudo-magnetogram reconstruction from CaII data prior to 1974. It can be used to estimate the amount of magnetic energy available for flares using scaling laws derived from observations (Crosby, Aschwanden, and Dennis, 1993; Shimizu and Tsuneta, 1997; Krucker and Benz, 1998; Parnell and Jupp, 2000) or from MHD models (Aulanier *et al.*, 2013). Toriumi *et al.* (2017) defined a proxy to estimate the flare energy from bright ribbons observed in H $\alpha$ .

Long-term archives can suffer from various artifacts (*e.g.* over-exposure, aging and defaults, lack of photometric calibration, missing temporal coverage). This can limit the analysis of the data and the robustness of the results. Chatzistergos *et al.* (2018) recently proposed a new method for automated processing and photometric calibration of CaII spectroheliograms. This method makes it possible to consistently combine and process images from different instruments and observatories, in order to build datasets with better temporal coverage. Such a method will be valuable for reconstructions of the solar irradiance (Fontenla *et al.*, 2011; Lean, 2018) for investigating long-term evolution and possible impact on Earth's climate (see the review by Haigh, 2007).

In this context, the 2018 upgrade of the Meudon spectroheliograph has two major goals:

- i) improve the spectroscopic capabilities of the instrument (better spectral and spatial sampling, better wavelength centering of images)
- ii) develop the scientific potential by providing full line profiles over the entire Sun and adding new lines such as CaII H (later CaII infrared), allowing thermodynamical diagnostics

### 3. Historical Background of the Meudon Spectroheliograph

The rapid expansion of spectroscopy began 150 years ago. In 1868, Janssen and Lockyer made the famous discovery of helium through observation of the HeI D3 587.5 nm line in the chromosphere. In 1869, Young discovered the "coronium" (FeXIV green line identified 70 years later) in eclipse spectra. These results (see Secchi, 1875, for the detailed history) initiated the development of solar spectroscopy, leading to the spectroheliograph invention in 1892 by two astronomers in France and USA (Hale, 1907; Deslandres, 1909).

The basic idea of spectroheliographs is to produce monochromatic images of the solar photosphere and chromosphere using narrow bandpass spectroscopic scans of strong Fraunhofer lines. For that purpose, the Meudon spectroheliograph was characterized by:

- a motorized objective (geographical E-W translation) moving the solar image over the entrance slit of the spectrograph

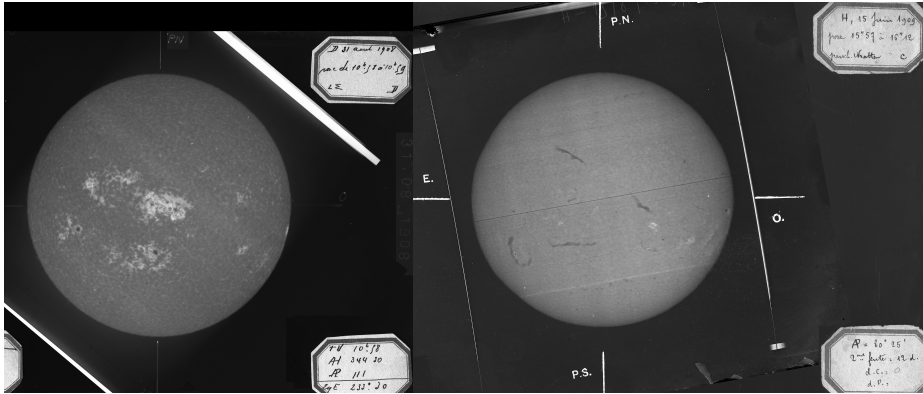


**Figure 1.** The Meudon collection of systematic CaII K and H $\alpha$  spectroheliograms started respectively in 1908 and 1909 (here images of 31 August 1908, and 15 June 1909)

- dispersive elements (prisms and, later, gratings)
- a curved slit in the spectrum isolating the chosen spectral line
- a motorized photographic plate in the spectrum moving at the same speed as the imaging objective
- an occulting disk in the solar image to produce deep scans for prominences

The first full-disk spectroheliograms were obtained by Deslandres at the Paris Observatory in 1894 using the CaII K line with glass photographic plates (85.4 mm solar diameter). The first long-exposure scans for prominences at the limb, using a disk attenuator, were got at the same time. Deslandres moved from Paris to Meudon in 1898 and a new laboratory and instrument were completed in 1906, with the collaboration of D’Azambuja (1920), who organized the solar-observation routines.

Systematic observations started in 1908 for CaII K and in 1909 for H $\alpha$  (Figure 1). The optics and mechanics were modernized in 1985 by Olivieri. Photographic plates were abandoned in 2001. The spectroheliograph no longer uses a selecting slit in the spectrum, and the moving plate is replaced by a fixed electronic detector. The 100,000 plates of the photographic collection are progressively being digitized. Weather conditions in Meudon allow at least one daily observation between 250 and 300 days per year.

#### 4. The 2018 Version of the Spectroheliograph

As in previous versions, the solar light feeding the spectrograph (Figure 2) is captured by a coelostat (two 400 mm flat mirrors) and directed horizontally towards a 250 mm doublet (O1, 4000 mm focal length). It is optimized for the red (656 nm) and violet (394 nm) part of the spectrum and forms a 37.2 mm solar image on the slit of the spectrograph. For other wavelengths, O1 can be translated to adjust the focus. A diaphragm reduces the entrance pupil to 170 mm, providing a theoretical resolution of 1'' in the red part of the spectrum.

In practice, this resolution is reduced to  $2''$  (or more) by local atmospheric turbulence.

The slit of the spectrograph has a width of 30 microns ( $1.5''$  on the Sun). The entrance objective O1 is motorized, so that the solar image moves slowly in the geographic E–W direction (scanning the full Sun typically takes 60 seconds). This motion decreases the resolution from  $1.5''$  to  $2''$ , but there is no consequence on image quality, due to seeing conditions.

The focal length of the collimator O2 is 1300 mm. This doublet is fixed and optimized for 656 and 394 nm; for other wavelengths, we insert into the beam a compensating plate.

The dispersion device is a grating (300 grooves/mm and  $17^{\circ}27'$  blaze angle). Incident and diffraction angles are respectively  $7^{\circ}$  and  $27^{\circ}$ . The interference order (3, 4, 5) is selected by filters behind the image plane (respectively 650, 500, 400 nm CWL and 78, 55, 66 nm FWHM). The wavelength switching is automatic and takes one minute.

In the present instrument, the camera lens O3 is an achromatic SkyWatcher 80ED, 400 mm focal length, forming a 11.4 mm image on the detector. The new camera uses a Fairchild 2020 scientific CMOS sensor with rolling electronic shutter. It is water cooled at  $5^{\circ}$  C. This is a low-noise device with 30,000 dynamic range and 16 bits digitization (0.5 electron per count). The format is  $2048 \times 2048$  square pixels (6.5 microns, 30,000 electrons full-well capacity). High speed readout (100 frames per second) allows fast spectroscopy. The quantum efficiency is for CaII H/K, H $\beta$ , and H $\alpha$  respectively 20 %, 65 %, and 70 %.

The spectral range is line-dependant. It usually varies from 40 to 100 pixels (typically 0.5 nm to 1.0 nm, see Table 1) and can be much enlarged (up to 10 nm) for specific programs upon request. The Sun is scanned using 2048 steps. The final angular pixel is  $1.1''$  (half of the best seeing at Meudon) with 3 % seasonal fluctuation in km.

The exposure time is chosen to work at half saturation in the far line wings (photon S/N ratio 100). It varies from 10 to 100 ms depending on line, disk attenuator, weather conditions, and height of the Sun. 10 ms is typically used for H $\alpha$ , 20 ms for CaII H/K and 50 ms for prominences with disk attenuator (20 to 100 seconds scan duration). The speed of objective O1 is automatically adjusted to the exposure time.

Two kinds of observations are performed daily:

- i) full-disk observations with short exposure time
- ii) prominence observations with solar disk attenuated by an occulter of neutral density 0.9 (13 % transmission) in the image plane (this avoids disk saturation of long exposure scans)

H $\alpha$ , H $\beta$ , and CaII are observed successively (but CaII H and K are simultaneous) in interference orders 3, 4, and 5. Figure 3 shows typical spectra  $P_{\text{obs}}(\lambda)$  obtained near disk center. The comparison with the atlas  $P_{\text{ref}}(\lambda)$  by Delbouille, Roland, and Neven (1973) recorded at the Jungfraujoch observatory (3600 m) with exceptional spectral resolution (0.2 pm) shows that lines are smoothed, as the spectroheliograph is designed for broad lines. A linear fit in the form

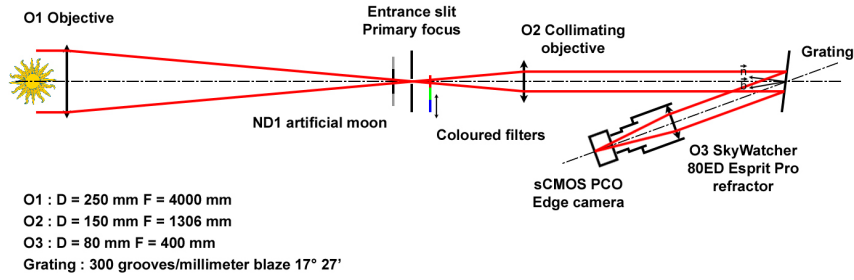


**Figure 2.** Optical design of the 2018 version of the spectroheliograph

**Table 1.** List of observable lines

Line	Wavelength [nm]	Order	Spectral Pix. [nm]	Spectral Res. [nm]	Spectral field [pixels]
H $\alpha$	656.28	3	0.0155	0.025	40
H $\beta$	486.13	4	0.0116	0.019	40
CaII H	396.85	5	0.0093	0.015	100
CaII K	393.37	5	0.0093	0.015	100

$P_{\text{obs}}(\lambda) = a + b \times P_{\text{ref}}(\lambda)$  reveals in line cores a small amount of stray or parasitic light (a few %).

MP4 movies are included as Electronic Supplemental Material to illustrate the principle of the 2018 version of the spectroheliograph (see the Appendix for details). At the moment, H $\beta$  is not yet operating, so that daily observations consist of one or several series of four sequences including:

- i) H $\alpha$  full-disk (short exposure)
- ii) H $\alpha$  prominences + disk attenuator (long exposure)
- iii) CaII H and K full-disk (short exposure)
- iv) CaII H and K prominences + disk attenuator (long exposure)

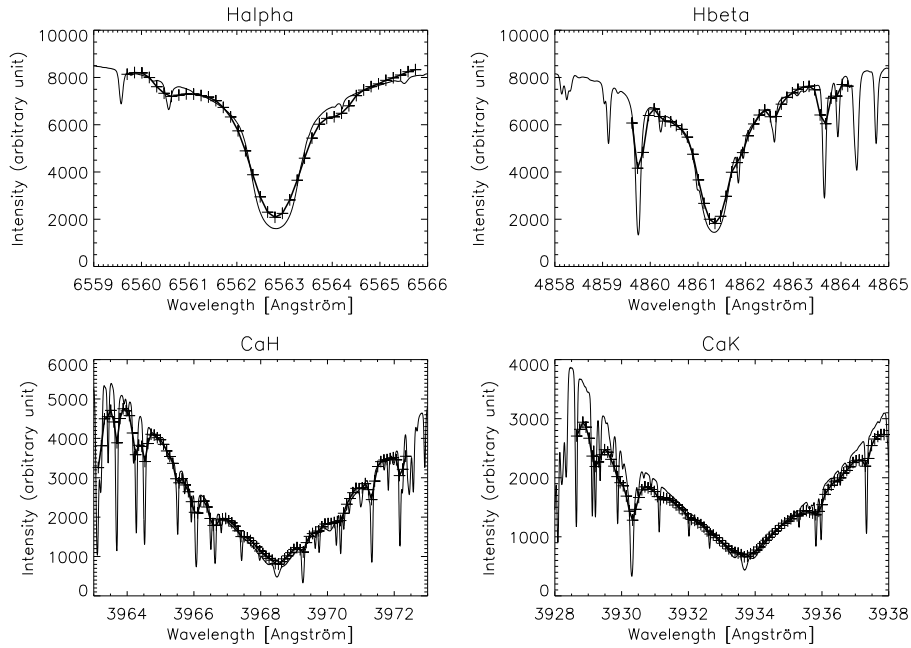


**Figure 3.**  $H\alpha$ ,  $H\beta$ , CaII H and CaII K line profiles near disk center (*thick line*) in comparison with atlas profiles, from Delbouille, Roland, and Neven (1973) (*thin line*). Sampling points are indicated by crosses.

$H\alpha$  line profiles allow the computation of Dopplergrams, as shown by Figure 4. We used a gaussian fit to detect the wavelength position of the line, but other methods working well with similar spectral resolutions may be used, as the bisector applied by Mein (1977) to multichannel subtractive double pass observations.

## 5. Data Levels and Dissemination

We offer to the solar community two data levels:

- i) Level 0: raw data cubes, in TIFF format available via anonymous FTP and dispatched in monthly catalogues at:

<ftp://ftpbass2000.obspm.fr/pub/meudon/spc/tiff/>

- ii) Level 1: data issued from a standard procedure and delivered by the solar database at:

<http://bass2000.obspm.fr/home.php?lang=en>

### 5.1. Level 0 Data

Level 0 data are 3D raw data containing 2048 planes of spectral images ( $x, \lambda$ ) resulting from the solar scan in the  $y$ -direction, except for the dark currents

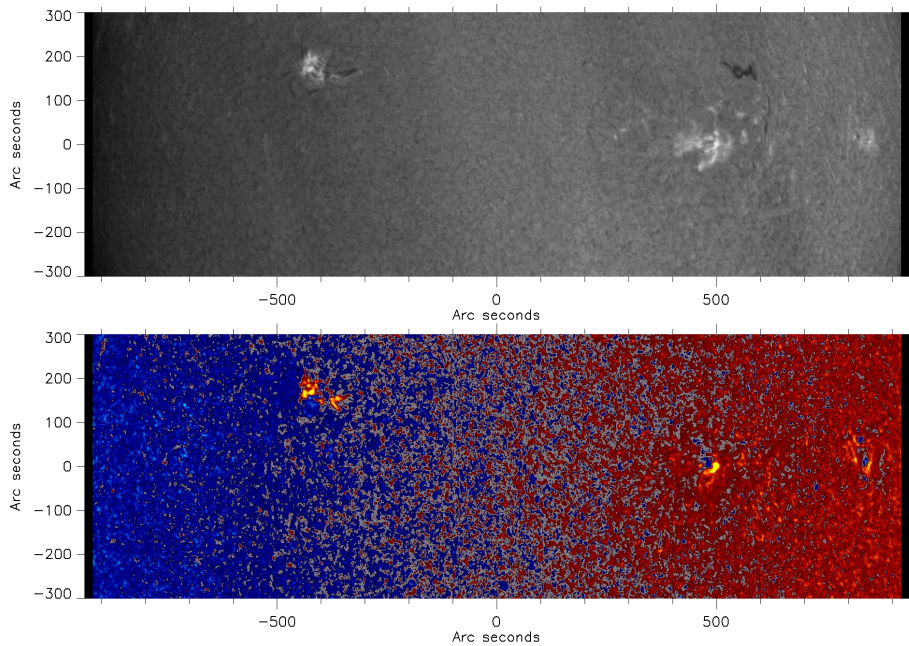


**Figure 4.**  $H\alpha$  intensitygram (top) and dopplergram (bottom) showing solar rotation, AR12715 (left) and AR12713 (right), 20 June 2018, 08:44 UT. Intensities are not uniform because of transparency variation.

(DC), which are 2D images. DC can be directly subtracted from each plane of the 3D raw observations.

More technical details and the IDL code to read raw data and reorder coordinates to produce  $(x, y, \lambda)$  datacubes are available here:

<http://observations-solaires.obspm.fr/Meudon-spectroheliograph-2018-version>

## 5.2. Level 1 Data

Level 1 is the result of a standard processing applied to level 0 data, including DC subtraction, correction of the spectral line curvature (parabolic fit), rotation (P-angle and coelostat position) in order to present the solar North at the top of the image.

Level 1 delivers FITS 3D output containing full line profiles  $(x, y, \lambda)$ , classical full-disk images (FITS for scientific purpose and quick look JPEG) and a set with superimposition of heliographic grids or polar angle graduations.

The optical procedure to produce flat fields is complicated and under development. It will be applied in Level 1 when available. Turbulence effects vary along the scan. Also, as the scanning and spectra acquisition speeds cannot be exactly equal, a residual distortion between geographic N–S and E–W may exist. It could be corrected using the method proposed by Mein and Ribes (1990).

Classical images (Figure 5) usually derived from line profiles are:

- i) CaII H3 and K3 line core (full-disk and prominences with attenuator)

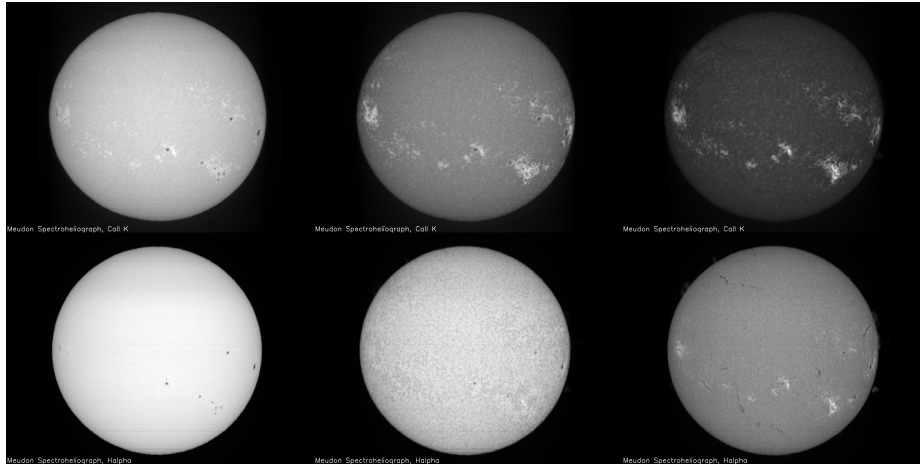


**Figure 5.** Example of images derived from profiles. **Bottom:**  $H\alpha$  -0.15 nm, -0.05 nm, center. **Top:**  $Ca II K$  -0.15 nm, -0.05 nm, center (tests of November 13, 2013)

**Table 2.** Spectroheliograph versions

Version	Spatial pixel [arcsec]	Spectral FOV [pixels]	Spectral pix. CaK- $H\alpha$ [nm]	Dynamic range [half sat.]	O3 f [mm]	output slit [ $\mu$ ]
PHOTO 1908–2001	1.5	1	0.015–0.025	density 3	3000	75
CCD 2002–2017	1.6	5	0.015–0.025	7500	900	
SCMOS 2018–	1.1	40–100 typical 1000 max	0.009–0.015	15000	400	

- ii)  $Ca II H1v$  and  $K1v$  violet wing (-0.15 nm apart from line center)
- iii)  $H\alpha$  line core (full-disk and prominences with attenuator)
- iv)  $H\alpha$  line wings (-0.05 and +0.05 nm apart from line center)
- v)  $H\alpha$  blue continuum (-0.15 nm apart from line center)

## 6. Discussion

The Meudon spectroheliograph is designed for full-disk observations of broad lines such as hydrogen or calcium. The characteristics of successive versions are summarized in Table 2.

The photographic version (image diameter 85.4 mm, 1908–1981 on  $10 \times 13$  cm glass plates and 1982–2001 on  $13 \times 18$  cm film plates) is affected by defaults that are discussed by Mein and Ribes (1990). The curved slit in the spectrum (75 microns width) was removed with the first CCD (2002–2017)

providing 5 wavelengths around line core. With this shutterless frame transfer CCD, a small amount of parasitic light differentially affects the five wavelengths during the transfer. Full line profiles are available since 2018 with a fast sCMOS sensor, which suppresses this phenomenon and has better spectral resolution and improved dynamic range. Scanning distortions still exist.

The 2018 upgrade allows the production of monochromatic images that are more precisely centered in wavelength, with smaller bandwidth, and better spatial sampling than before. Wavelength centering is now done by computer, while in the former version, it was by visual inspection. Line inclination and curvature are now corrected (Level 1 data only).

The availability of full line profiles is the major change since 1908. It is now possible to derive dopplergrams of active regions in  $H\alpha$ . The spectral range is broad (0.5 nm or more), so that large velocities can be recorded. Filament tracking, which may be affected by Doppler shifts, is improved. The spectroheliograph can follow dynamic events such as flares or eruptive filaments, with moderate temporal resolution (a few minutes) in the case of full-disk scan. A faster mode is implemented for active regions (reduced FOV). However, continuous observations cannot be systematic, because of personnel limitations and meteorological conditions, but participation in flare campaigns is possible.

Many parameters (temperature, velocity, and their gradients) can be extracted from CaII line profiles. Mein *et al.* (1987) proposed a non-linear method based on Fourier series. Disturbances of Fourier coefficients were compared to theoretical disturbances of atmospheric models. Corresponding line profiles were computed using a NLTE radiative transfer code. Temperature and velocity fluctuations, together with vertical gradients, were derived from a least-square inversion method. It was applied successfully to a time sequence of CaII 396.8 nm line. Blue peaks occurring in profiles were interpreted as downward velocity gradients associated with temperature enhancement. Molowny-Horas *et al.* (1999) used another NLTE code to build a grid of  $H\alpha$  lines and inverted observed profiles of filaments. Mein *et al.* (2000) made a cloud model to fit CaII 854.2 nm profiles also in the case of filaments. More recently, Beck *et al.* (2015) presented a fast inversion code for CaII 854.2 nm. It is based on an archive of theoretical spectra that are computed under the assumption of LTE. From a comparison to NLTE inversions, they applied a first-order correction to the parameters deduced from the LTE case. Kuridze *et al.* (2017) also produced inversions of the CaII 854.2 nm line using a NLTE code to investigate the evolution of temperature and velocity in the flaring chromosphere.

For these reasons, systematic observation of CaII infrared lines are planned for the Meudon spectroheliograph.

## 7. Conclusion

The 2018 upgrade of the Meudon spectroheliograph marks a major change since 1908. It provides full line profiles over the entire solar disk, with good spectral sampling (0.010 nm to 0.015 nm) over a 1 nm typical spectral field (up to 10 nm upon request). 3D data cubes ( $x, y, \lambda$ ) are now produced daily, together with

classical images at different wavelenths along the profiles.  $H\alpha$ , CaII H, and K lines are routinely observed;  $H\beta$  and CaII infrared lines will come later. Both Level 0 (raw) and 1 data are available on-line to the community.

Spectra observed with the spectroheliograph are good indicators of solar activity in the chromosphere (active regions, faculae, filaments, prominences), while activity in the transition region and corona is provided by Solar Dynamics Observatory (Atmospheric Imaging Assembly, AIA). The 160 and 170 nm continua observed by AIA at the top of the photosphere give images close to CaII (except for filaments), so that combined ground-based and space observations produce a complete diagnostic of the solar atmosphere.

The main scientific objective of the Meudon spectroheliograph, with a few series of daily observations, concerns long-term solar activity, rare and extreme events, and the continuation of the ten solar cycles collection. CaII retraces the history of the surface covered by magnetic fields, and  $H\alpha$  records chromospheric phenomena. Line profiles open new perspectives in terms of temperature and velocity determination by inversion techniques.

Data before 2002 (images in CaII K3, K1v, and  $H\alpha$ ) are registered on photographic media (glass or film) and scanned. We intend to recover the production of synoptic maps using automated procedures (Abouadarham *et al.*, 2008).

A complementary short-term and automatic survey at high temporal resolution (20 seconds) for observations of transient activity (fares, filament eruption, CME onset, Moreton waves) is under development for the Calern Observatory using monochromatic  $H\alpha$  and CaII K filters; this will be the topic of a later article.

*If you use data for publication, please insert the following acknowledgment: “Meudon spectroheliograph data are courtesy of the solar and BASS2000 teams, as part of operational services of Paris Observatory”*

**Acknowledgments** This article is dedicated to the memory of E. Ribes who directed Meudon solar observations during many years and passed away prematurely in 1996.

We thank the referee for helpful comments and suggestions. We are also indebted to the technical staff of LESIA (D. Crussaire, N. Füller, C. Imad, M. Ortiz, C. Renié and D. Ziegler) and to the team of observers which operate daily the instrument (C. Blanchard, I. Bualé, S. Cnudde, A. Docclo, I. Ibntaieb). We are grateful to the Scientific Council of Paris Observatory for financial support and INSU/CNRS for the label of National Observing Service (SNO). K.D. is supported by the Centre National d’Etudes Spatiales (CNES).

## Disclosure of Potential Conflicts of Interest

The authors declare that they have no conflicts of interest.

## Appendix

Electronic Supplemental Material (movies in MPEG 4 format).

- i) Movie 1: the principle of the 2018 upgrade of the Meudon spectroheliograph in the case of CaII K line. The surface of the Sun (right) is scanned by a thin slit and full line profiles (left) are recorded for the 2048 positions of the slit. Data are stored in 3D files (2 space coordinates + spectral line). The scan time takes about 60 seconds using a 1.5'' slit.
- ii) Movie 2: same as Movie 1, but for H $\alpha$  line.
- iii) Movie 3: example of images got at different wavelength positions along the line profiles. Part 1: H $\alpha$  ; Part 2: CaII K.

## References

- Aboudarham, J., Scholl, I., Fuller, N., Fouesneau, M., Galametz, M., Gonon, F., Maire, A., Leroy, Y.: 2008, Automatic detection and tracking of filaments for a solar feature database. *Ann. Geophys.* **26**, 243. DOI. ADS.
- Aulanier, G., Démoulin, P., Schrijver, C.J., Janvier, M., Pariat, E., Schmieder, B.: 2013, The standard flare model in three dimensions. II. Upper limit on solar flare energy. *Astron. Astrophys.* **549**, A66. DOI. ADS.
- Beck, C., Choudhary, D.P., Rezaei, R., Louis, R.E.: 2015, Fast Inversion of Solar Ca II Spectra. *Astrophys. J.* **798**, 100. DOI. ADS.
- Bertello, L., Ulrich, R.K., Boyden, J.E.: 2010, The Mount Wilson Ca ii K Plage Index Time Series. *Solar Phys.* **264**, 31. DOI. ADS.
- Carrington, R.C.: 1859, Description of a Singular Appearance seen in the Sun on September 1, 1859. *Mon. Not. Roy. Astron. Soc.* **20**, 13. DOI. ADS.
- Charbonneau, P.: 2010, Dynamo Models of the Solar Cycle. *Liv. Rev. Solar Phys.* **7**, 3. DOI. ADS.
- Chatzistergos, T., Ermolli, I., Solanki, S.K., Krivova, N.A.: 2018, Analysis of full disc Ca II K spectroheliograms. I. Photometric calibration and centre-to-limb variation compensation. *Astron. Astrophys.* **609**, A92. DOI. ADS.
- Crosby, N.B., Aschwanden, M.J., Dennis, B.R.: 1993, Frequency distributions and correlations of solar X-ray flare parameters. *Solar Phys.* **143**, 275. DOI. ADS.
- D’Azambuja, L.: 1920, Le Spectroheliographe. *L’Astronomie* **34**, 487. ADS.
- Delbouille, L., Roland, G., Neven, L.: 1973, *Atlas photometrique du spectre solaire de [lambda] 3000 a [lambda] 10000*, Université de Liège. ADS.
- Deslandres, H.: 1909, On the progressive revelation of the entire atmosphere of the Sun. *The Observatory* **32**, 282. ADS.
- Ellison, M.A.: 1946, Visual and spectrographic observations of a great solar flare, 1946 July 25. *Mon. Not. Roy. Astron. Soc.* **106**, 500. DOI. ADS.
- Fontenla, J.M., Harder, J., Livingston, W., Snow, M., Woods, T.: 2011, High-resolution solar spectral irradiance from extreme ultraviolet to far infrared. *J. Geophys. Res. (Atmos.)* **116**, D20108. DOI. ADS.
- Gallagher, P.T., Denker, C., Yurchyshyn, V., Spirock, T., Qiu, J., Wang, H., Goode, P.R.: 2002, Solar activity monitoring and forecasting capabilities at Big Bear Solar Observatory. *Ann. Geophys.* **20**, 1105. DOI. ADS.
- Garcia, A., Sobotka, M., Klvaňa, M., Bumba, V.: 2011, Synoptic observations with the Coimbra spectroheliograph. *Contr. Astron. Obs. Skalnaté Pleso* **41**, 69. ADS.
- Haigh, J.D.: 2007, The Sun and the Earth’s Climate. *Liv. Rev. Solar Phys.* **4**, 2. DOI. ADS.
- Hale, G.E.: 1907, Some New Applications of the Spectroheliograph. *Astrophys. J.* **25**, 311. DOI. ADS.
- Hale, G.E., Ellerman, F., Nicholson, S.B., Joy, A.H.: 1919, The Magnetic Polarity of Sun-Spots. *Astrophys. J.* **49**, 153. DOI. ADS.
- Harvey, J.W., Bolding, J., Clark, R., Hauth, D., Hill, F., Kroll, R., Luis, G., Mills, N., Purdy, T., Henney, C., Holland, D., Winter, J.: 2011, Full-disk Solar H-alpha Images From GONG. In: *AAS/Solar Phys. Div. Abs. #42*, *Bull. Am. Astron. Soc.* **43**, 17.45. ADS.

- Hasan, S.S., Mallik, D.C.V., Bagare, S.P., Rajaguru, S.P.: 2010, Solar Physics at the Kodaikanal Observatory: A Historical Perspective. *Astrophys. Space Sci. Proc.* **19**, 12. DOI. ADS.
- Hathaway, D.H.: 2010, The Solar Cycle. *Living Reviews in Solar Physics* **7**, 1. DOI. ADS.
- Hathaway, D.H., Wilson, R.M., Reichmann, E.J.: 2002, Group Sunspot Numbers: Sunspot Cycle Characteristics. *Solar Phys.* **211**, 357. DOI. ADS.
- Hodgson, R.: 1859, On a curious Appearance seen in the Sun. *Mon. Not. Roy. Astron. Soc.* **20**, 15. DOI. ADS.
- Hoyt, D.V., Schatten, K.H.: 1998, Group Sunspot Numbers: A New Solar Activity Reconstruction. *Solar Phys.* **181**, 491. DOI. ADS.
- Karna, N., Pesnell, W.D., Zhang, J.: 2015, A comprehensive study of cavities on the Sun: Structures and Evolution. In: *AGU Fall Meet. Abs.* **2015**, SH54B. ADS.
- Krucker, S., Benz, A.O.: 1998, Energy Distribution of Heating Processes in the Quiet Solar Corona. *Astrophys. J.* **501**, L213. DOI. ADS.
- Kuridze, D., Henriques, V., Mathioudakis, M., Koza, J., Zaqarashvili, T.V., Rybák, J., Hansmeier, A., Keenan, F.P.: 2017, Spectroscopic Inversions of the Ca II 8542 Å Line in a C-class Solar Flare. *Astrophys. J.* **846**, 9. DOI. ADS.
- Lean, J.L.: 2018, Estimating Solar Irradiance Since 850 CE. *Earth Space Sci.* **5**, 133. DOI. ADS.
- Leroy, J.L., Bommier, V., Sahal-Brechot, S.: 1983, The magnetic field in the prominences of the polar crown. *Solar Phys.* **83**, 135. DOI. ADS.
- Makarov, V.I., Sivaraman, K.R.: 1989, New Results Concerning the Global Solar-Cycle. *Solar Phys.* **123**, 367. DOI. ADS.
- Martres, M.-J., Zlicaric, G.: 1982, L'activité solaire, cartes synoptiques de la chromosphere et des taches. *L'Astronomie* **96**, 45. ADS.
- Mein, P.: 1977, Multi-channel subtractive spectrograph and filament observations. *Solar Phys.* **54**, 45. DOI. ADS.
- Mein, P., Ribes, E.: 1990, Spectroheliograms and motions of magnetic tracers. *Astron. Astrophys.* **227**, 577. ADS.
- Mein, P., Mein, N., Malherbe, J.M., Dame, L.: 1987, Inversion of line profile disturbances - A nonlinear method applied to solar CaII lines. *Astron. Astrophys.* **177**, 283. ADS.
- Mein, P., Briand, C., Heinzel, P., Mein, N.: 2000, Solar arch filaments observed with THEMIS. *Astron. Astrophys.* **355**, 1146. ADS.
- Molowny-Horas, R., Heinzel, P., Mein, P., Mein, N.: 1999, A non-LTE inversion procedure for chromospheric cloud-like features. *Astron. Astrophys.* **345**, 618. ADS.
- Mouradian, Z., Soru-Escout, I.: 1993, On solar activity and the solar cycle. A new analysis of the Butterfly Diagram of sunspots. *Astron. Astrophys.* **280**, 661. ADS.
- Mouradian, Z., Soru-Escout, I.: 1994, A new analysis of the butterfly diagram for solar filaments. *Astron. Astrophys.* **290**, 279. ADS.
- Norton, A.A., Charbonneau, P., Passos, D.: 2014, Hemispheric Coupling: Comparing Dynamo Simulations and Observations. *Space Sci. Rev.* **186**, 251. DOI. ADS.
- Parnell, C.E., Jupp, P.E.: 2000, Statistical Analysis of the Energy Distribution of Nanoflares in the Quiet Sun. *Astrophys. J.* **529**, 554. DOI. ADS.
- Petrovay, K.: 2010, Solar Cycle Prediction. *Liv. Rev. Solar Phys.* **7**, 6. DOI. ADS.
- Pevtsov, A.A., Virtanen, I., Mursula, K., Tlatov, A., Bertello, L.: 2016, Reconstructing solar magnetic fields from historical observations. I. Renormalized Ca K spectroheliograms and pseudo-magnetograms. *Astron. Astrophys.* **585**, A40. DOI. ADS.
- Ribes, E., Bonfond, F.: 1990, Magnetic tracers, a probe of the solar convective layers. *Geophys. Astrophys. Fluid Dyn.* **55**, 241. DOI. ADS.
- Schmieder, B.: 2018, Extreme solar storms based on solar magnetic field. *J. Atmos. Solar-Terr. Phys.* **180**, 46. DOI. ADS.
- Schrijver, C.J., Beer, J., Baltensperger, U., Cliver, E.W., Güdel, M., Hudson, H.S., McCracken, K.G., Osten, R.A., Peter, T., Soderblom, D.R., Usoskin, I.G., Wolff, E.W.: 2012, Estimating the frequency of extremely energetic solar events, based on solar, stellar, lunar, and terrestrial records. *J. Geophys. Res. (Space Phys.)* **117**, A08103. DOI. ADS.
- Schwabe, H.: 1844, Sonnenbeobachtungen im Jahre 1843. Von Herrn Hofrath Schwabe in Dessau. *Astron. Nach.* **21**, 233. DOI. ADS.
- Secchi, A.: 1875, *Le Soleil*. DOI. ADS.
- Shimizu, T., Tsuneta, S.: 1997, Deep Survey of Solar Nanoflares with Yohkoh. *Astrophys. J.* **486**, 1045. DOI. ADS.

- Tobias, S.M.: 2002, The solar dynamo. *Phil. Trans. of the Roy. Soc. London Series A* **360**, 2741. DOI. ADS.
- Toriumi, S., Schrijver, C.J., Harra, L.K., Hudson, H., Nagashima, K.: 2017, Magnetic Properties of Solar Active Regions That Govern Large Solar Flares and Eruptions. *Astrophys. J.* **834**, 56. DOI. ADS.
- Wolf, R.: 1861, Abstract of his latest Results. *Mon. Not. Roy. Astron. Soc.* **21**, 77. DOI. ADS.